Lattice distortion in hcp rare gas solids

A. Grechnev, S.M. Tretyak, and Yu.A. Freiman

B. Verkin Institute for Low Temperature Physics and Engineering of the National Academy of Sciences of Ukraine
47 Lenin Ave., Kharkov 61103, Ukraine
E-mail: shrike4625@yahoo.com

The lattice distortion parameter $\delta \equiv c/a - \sqrt{8/3}$ has been calculated as a function of molar volume for the hcp phases of He, Ar, Kr, and Xe. Results from both semi-empirical potentials and density functional theory are presented. Our study shows that δ is negative for helium in the entire pressure range. For Ar, Kr, and Xe, however, δ changes sign from negative to positive as the pressure increases, growing rapidly in magnitude at higher pressures.

1. Introduction

Rare gases (He, Ne, Ar, Kr, Xe, and Rn) crystallize in the most closely packed structures: the face-centered cubic (fcc) and the hexagonal close-packed (hcp). Solid helium has hcp structure at low pressures and it has been demonstrated experimentally that it stays in this structure up to at least 57 GPa [1], apart from narrow bcc and fcc areas at the melting line. On the other hand, heavier rare gas solids (RGS's) have fcc structure at low pressures. Under pressure, Ar [2], Kr [3], and Xe [4] have been found experimentally to change into the hcp structure, while neon stays fcc [5]. It has been shown in our previous paper [6] that the hcp structure of solid He is stabilized by strong zero-point vibrations.

The c/a ratio of the hcp RGS's is very close to the ideal value $\sqrt{8/3} \approx 1.633$. The deviation of the c/a ratio from the ideal value is described by the lattice distortion parameter $\delta \equiv c/a - \sqrt{8/3}$. If $\delta > 0$, the lattice is elongated along the z axis, if $\delta < 0$, then it is contracted along the z axis. The point $\delta = 0$ ($c/a = \sqrt{8/3}$) corresponds to the packing of hard spheres. In the case of crystals with c/a different from $\sqrt{8/3}$, the lattice has exactly the same symmetry as the ideal hcp lattice, i.e., the space groups of these crystals are identical for all values of c/a. While most physical properties of the hcp solids are not very sensitive to the c/a ratio (for a given volume), δ determines the second-order contributions to the crystal field held (as shown for solid H_2 in Ref. 7), which is zero for the ideal hcp lattice. It is interesting to note that δ is

negative for all metallic elemental hcp solids except Zn and Cd. Our previous calculations [6] show that for hcp He δ is negative in a wide range of pressures.

While there have been numerous experimental attempts to determine c/a in helium (see the references and discussion in Ref. 6), the results for heavier RGS's are very scarce. The x-ray diffraction studies of Xe by Caldwell et al. [8] and Jephcoat et al. [4] find δ to be positive under pressure (although the experimental precision was not sufficient to prove this fact unambiguously). On the theoretical side, there have been several papers devoted to the calculation of the c/a ratio for Ar, Kr, and Xe, however the results are also somewhat controversial. Schwerdtfeger et al. [9] investigated rare gas solids with a number of different extended van der Waals pair potentials and found $\delta < 0$ for hcp He, Ne, Ar, and Kr for all potentials at zero pressure. Caldwell et al. [8] and Yao and Tse [10] used density functional theory (DFT) and found $\delta > 0$ for Xe, while Cohen et al. [11] reported negative δ for Xe, also within the framework of DFT. It seems that we still know very little about the c/a ratio in hcp rare gas solids in the age when all structural properties of most elemental solids (including high-pressure phases) are firmly established from both theory and experiment.

In an attempt to clarify this issue, in the present paper we calculate the lattice distortion parameter δ for hcp Ar, Kr, and Xe as a function of volume. In addition, we also present results for He, which are the extension of our previous calculations [6]. Unfortunately, we are aware of no single theoretical method which gives an accurate δ for

RGS's both at low pressures and at very high pressures (of the order of the metallization point). The reason for this is the different nature of the chemical binding of RGS's (and other molecular crystals) for different pressures. At low pressures, an RGS is a crystal with pure molecular binding, held together by the van der Waals forces. At higher pressures, the binding becomes more covalent in character, and finally metallic above the metallization point. That is why we use two methods in the present paper: semi-empirical potentials [12–14] and the density functional theory (DFT) [15,16].

The semi-empirical (SE) potentials (with pair and triple forces included) work very well at low pressures, while for the higher pressures higher order n-body forces are important. In particular, the SE potentials become useless in the metallic phase (where the sum over n-body terms converges extremely slowly) or near the metallization point. Density functional theory is formally an exact theory, but for practical calculations one always needs some kind of a model expression for the electronic exchange-correlation energy as a functional of the electronic density. The most widely used approximations are the local density (LDA) and generalized gradient (GGA) approximations. They are routinely used nowadays to calculate various electronic and structural properties of all kinds of solids, including RGS's [8,10,17]. These approximations are expected to be rather accurate at high pressures around the metallization point (as LDA and GGA are in general most suitable for metallic and covalent solids), but fail at low pressures due to the poor description of the van der Waals (vdW) interaction [18]. In other words, the two methods employed by us complement each other: one can use the semi-empirical approach for low pressures and DFT for higher pressures.

2. Method

2.1. Semi-empirical potentials

In our semi-empirical calculations we include pair (U_2) and triple (U_3) interatomic forces, therefore the expression for the total energy is $U_{\text{tot}} = U_2 + U_3$. The n-body interactions with $n > 3$ are not included, which makes the method accurate only at low pressures, as we discuss below in Sec. 3. We use the Aziz expression [19] for the pair potentials with parameters from Ref. 14. The three-body potential is taken as a sum of the long-range Axilrod–Teller dispersive interaction and the short-range three-body exchange interaction in the Slater–Kirkwood form [12–14]. We restrict ourselves to $T = 0$ K. The zero-point energy is treated approximately within the Einstein model. For the heavier RGS's this approximation is valid for the whole pressure range, but for helium we exclude the small pressure range (~ 0.1 GPa) where quantum-crystal effects play a decisive role. The exactly same model has been employed previously to calculate the equations of state for

all the RGS's [14], and the results are in excellent agreement with experiment.

Assuming that δ is small, we expand the ground state energy E_{gs} to the second order in δ:

$$E_{gs}(\delta) = b_0 + b_1\delta + b_2\delta^2, \qquad (1)$$

where the coefficients b_0, b_1, and b_2 depend on the molar volume and also on the parameters of the interatomic potential. The minimum of E_{gs} is reached for $\delta = -b_1/(2b_2)$. Thus, in order to find the $\delta(V)$ dependence one has to calculate the quantities $b_1(V)$ and $b_2(V)$. The first shell of neighbors gives the main positive contribution to b_2, and the sum over spheres of neighbors converges rather rapidly. However, despite the relatively short-range character of the interatomic interactions, one has to include a large number of neighbor shells in order to calculate b_1 accurately. The reason is that the contributions of the first two shells are exactly equal to zero, while the contributions from more distant shells decrease rather slowly and tend to alternate in signs. This is also the reason why δ is small, namely $|\delta| \sim 10^{-4} - 10^{-3}$ at low pressures. Note that the contributions to b_1 from nearest and next nearest neighbors vanish for different reasons. The contribution from the nearest neighbors in the xy plane exactly cancels the contribution from the nearest neighbors below and above the xy plane due to the equality of all the nearest neighbor distances for the ideal $c/a = \sqrt{8/3}$. Regarding the second shell, each of the six atoms in it gives zero contribution individually. The contribution to b_1 from the third shell (which contains only two atoms at the distance $R = a\sqrt{8/3}$ from the central atom) leads to $b_1 > 0$ resulting in $\delta < 0$. Additionally, 18 neighbors of the fourth shell at the distance $R = a\sqrt{3}$ makes a negative contribution to b_1 which overweights the positive contribution from the third shell. As a result, the total contribution to b_1 from the third and fourth shells is negative and leads to $\delta > 0$. The contributions from further shells will in most cases lead to $\delta < 0$. To get a reliable result, we take into account 50 shells of neighbors in all our calculations.

2.2. First principles calculations

For our DFT calculations we use the all-electron full-potential linear muffin-tin orbital (FP–LMTO) code RSPt [20,21]. This code is especially reliable for high-pressure calculations, as it uses the «soft-core approach», i.e., core electrons energies and wave functions are recalculated for each DFT iteration. This means that the core levels in a crystal, especially under pressure, are shifted from the atomic positions, giving more accurate total energy values. The generalized gradient approximation (GGA) in the form of Perdew–Burke–Ernzerhof (PBE) [22] has been used. All our calculations have been done for zero temperature neglecting the zero-point vibrations.

The equilibrium c/a ratio has been found for each molar volume V by minimizing the total energy $E(c/a)$ for fixed V. This function was calculated for a number of c/a points around the minimum and interpolated with a cubic spline. The equilibrium c/a and the energy $E(V)$ for the equilibrium c/a were then obtained from this spline. The pressure $p(V)$ (for the equation of state) was obtained from the calculated $E(V)$ points, again using a cubic spline for the numerical differentiation. We took special care in achieving high accuracy of our calculations, as the typical energy differences for He, between, say $c/a = 1.633$ and 1.634 are of the order of 10^{-6} to 10^{-9} Ry, depending on V (somewhat larger for the heavier elements). In particular, the Brillouin zone integration has been performed by the tetrahedron method with 368 k-points in the irreducible part of the Brillouin zone (3375 k-points in the whole Brillouin zone). The self consistent cycle was converged to the total energy accuracy of at least 10^{-9} Ry. We have used two kinetic energy tails with energies $+0.2$ Ry and -0.2 Ry respectively in our basis set; and the $32 \times 32 \times 32$ mesh for the Fast Fourier Transform in the real space. For Kr and Xe, a second energy set with two kinetic energy tails (-0.8 Ry and -1.5 Ry) has been used to describe $3d$- and $4d$-states, respectively. Our tests show that the results are basically insensitive to the particular choice of the kinetic energy tails and they are well converged with the number of k-points and other parameters of the calculation. We also applied LDA to helium and found out that the LDA results (not shown) are very close to our GGA results. In fact, we managed to achieve the numerical accuracy of at least $3 \cdot 10^{-4}$ in determining δ (this does not include the possible systematic errors of GGA and the FP–LMTO method).

It is important to note that DFT maps the many-body problem to an effective one-particle Scrödinger-like Kohn–Sham equation [16]. The periodic solids are treated in k-space using Bloch theorem. Compared to the real-space methods (like the semi-empirical potentials) it gives DFT an advantage of automatically including all shells of neighbors and all n-body interactions in its expression for the total energy. The main disadvantage of DFT within LDA or GGA for rare gas solids is, as we already mentioned, the poor description of the van der Waals interaction. Therefore, while this method is ideal for the metallic phase, and also suitable for the insulating phase in the vicinity of the metallization point, it does not give reliable results at low pressures, where an RGS behaves as a pure molecular crystal and the vdW interaction is important.

3. Results and discussion

In this section we present the results of our calculation. For reader's convenience, in Table 1 we list the experimental equilibrium molar volumes V_0 of rare gas solids (from Ref. 23). Note that V_0 for helium is high due to the
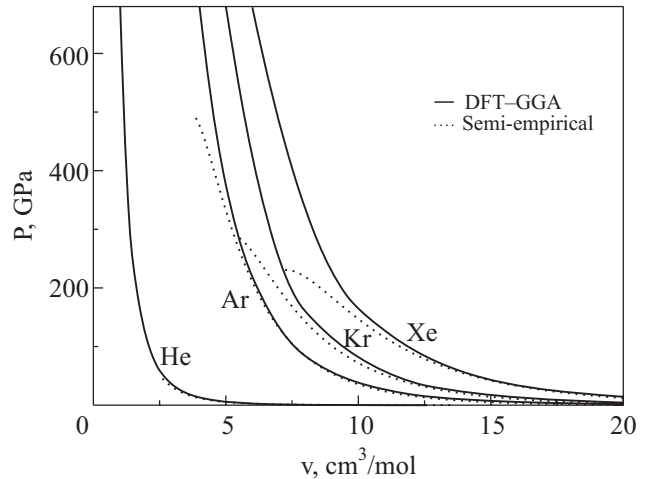

Fig. 1. The calculated equation of state for He, Ar, Kr, and Xe.

zero-point oscillations. In the same table, the theoretical metallization volumes V_{MET} from our calculations are presented. The metallization volume is typically somewhat overestimated by LDA/GGA (by about 20% for helium [24]), thus the metallization pressure is underestimated. This is a direct consequence of LDA/GGA underestimating the band gap in insulators.

Table 1. The experimental equilibrium molar volume V_0 (from Ref. 23, Ch. 13, p. 825, Table 1) and the theoretical metallization point V_{MET} (from our DFT–GGA calculations) for rare gas solids

	V_0, cm³/mol	V_{MET}, cm³/mol
He	21.0	0.228
Ar	22.56	4.42
Kr	27.10	6.48
Xe	34.74	10.9

The calculated equations of state for He, Ar, Kr, and Xe are presented in Fig. 1, again for the reader's convenience. The $p(V)$ curves for the equilibrium c/a virtually coincide with the $p(V)$ curves for the ideal c/a (not shown). One can see the breakdown of the semi-empirical picture at higher pressures due to the lack of the $n > 3$ terms in the n-body expansion.

3.1. Helium

The calculated lattice distortion parameter δ as a function of the molar volume V for hcp helium is shown in Fig. 1. This is an extension of our previous work on He [6] with more volume points included in the DFT–GGA calculation. First of all, the order of magnitude of δ is about 10^{-3} in a wide range of volumes (above 5 cm³/mol). This would be a very small effect for hcp metals, but it is an expected order of magnitude for molecular crystals.
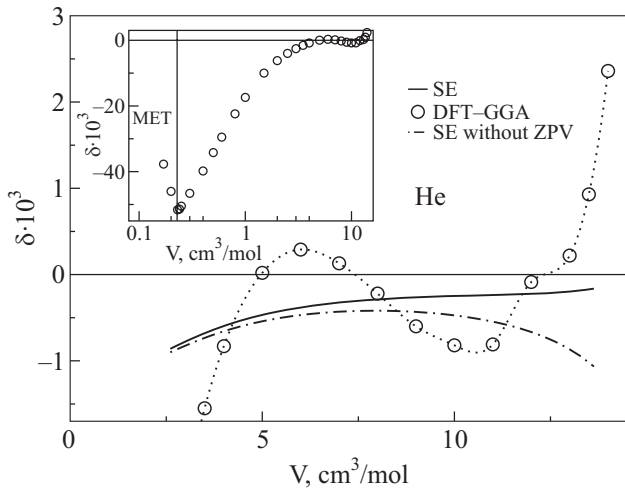
Fig. 2. The lattice distortion parameter δ for hcp helium as a function of molar volume V from DFT–GGA, SE potentials, and the semi-empirical results without ZPV. The circles are calculated DFT–GGA points, while the smooth dotted curve is a cubic spline. The inset shows the DFT–GGA data for small volumes.

The semi-empirical (SE) calculations without zero-point vibrations (dash-dotted curve) give negative δ in the entire volume range, with a maximum at about 8 cm³/mol. The negative sign is not unexpected, as most hcp solids have negative δ, at least at low pressures. At smaller volumes, negative δ grows in absolute value with decreasing volume (increasing pressure). It also grows sharply in absolute value when the volume approaches 14 cm³/mol. Note that the large equilibrium volume of solid helium (21.0 cm³/mol) and the preference of the hcp phase to fcc are effects of the zero-point vibrations (ZPV). If ZPV were not taken into account, helium at ambient conditions would be a solid with the fcc structure and molar volume of about 10 cm³/mol [25]. Therefore, when comparing helium to other rare gas solids (see the results below), the effective V_0 for He (without ZPV) should be placed at about 10 cm³/mol, but not 21.0 cm³/mol. Calculations without ZPV at $V > 10$ cm³/mol correspond to the hypothetical case of expanded lattice and energetically unfavourable hcp structure, so there is little surprise that the c/a ratio deviates from the ideal value at these volumes.

The picture changes drastically when the ZPV are included in the calculation (solid line in Fig. 1). At $V < 5$ cm³/mol the two curves practically coincide. However, the results with ZPV have no increase of the absolute value of δ at $V > 10$ cm³/mol. In fact, there is no maximum and δ grows monotonously with increasing V. It stays small in magnitude and possibly becomes positive at larger volumes. However, our calculations only include

ZPV in a rather simple way based on the Einstein model. For this reason, we do not present the results for volumes larger than 14 cm³/mol. The detailed examination of the quantum crystal region is beyond the scope of the present paper. In our previous paper [6] we have studied the effect of pair (2-body) and triple (3-body) forces on lattice distortion. It has been shown that the triple forces become important at approximately $V < 10$ cm³/mol. It is difficult to say exactly at what volumes the higher order terms (not included in the present SE calculations) come into play, but one can expect the SE description to be adequate between at least 10 and 14 cm³/mol (quite possibly down to 5 cm³/mol).

The DFT calculations (circles and the dotted curve in Fig. 2) report a negative δ at $V < 5$ cm³/mol, which grows in magnitude with decreasing V much quicker than is given by the SE potentials. The reason is that DFT automatically includes all n-body terms, while the SE method is limited by the 3-body terms and should not be used for $V < 5$ cm³/mol. For volumes above 5 cm³/mol, however, the δ from DFT behaves nonmonotonously and finally becomes positive and grows sharply at $V >> 11$ cm³/mol. We believe the latter region (and possibly even the entire region above 5 cm³/mol) to be nonphysical, as GGA is known to describe poorly the van der Waals (vdW) interaction. However, for $V < 4$ cm³/mol the DFT is expected to be reliable, as the atomic repulsive forces dominate in this high-pressure region and the vdW contribution is small. At very low volumes (which correspond to the experimentally unreachable pressures of thousands of GPa), δ reaches a minimal value of -0.05 at about 0.23 cm³/mol, which is very close to the metallization point (vertical line in the inset of Fig. 2). In the metallic phase, δ increases sharply (thus decreasing in the absolute value) with decreasing V.

To summarize, DFT–GGA works for $V < 4$ cm³/mol, while the SE potentials are expected to give adequate results between 10 and 14 cm³/mol. Unfortunately, one does not know what happens exactly between 4 and 10 cm³/mol, as DFT and SE give somewhat different results for this region. However, both methods provide a negative (or close to zero) δ of the order of 10^{-4}–10^{-3} for these «intermediate» volumes. So now it is up for the experimentalists to clarify this issue. It might be also tempting to apply one of the formally exact quantum mechanical methods, such as quantum Monte Carlo or configuration interaction, to this problem. However, these methods work with finite cluster, and as the lattice distortion is a very delicate effect (energy differences can be as small as 10^{-9} Ry), it would be very difficult to eliminate the finite cluster size errors and obtain a reliable result. For this reason we do not use these methods in the present paper.

3.2. Heavier rare gas solids

The $\delta(V)$ dependence for hcp argon is presented in Fig. 3. The two vertical lines correspond to the metallization point and the equilibrium volume, respectively (see Table 1). The SE results (solid curve) are qualitatively similar to the SE results for He (without ZPV). The effect of zero points vibrations in Ar and other heavier RGS's is very small and the SE curve without ZPV (not shown) practically coincides with the full SE curve. The lattice distortion parameter δ is negative with a maximum at about 15 cm³/mol. The DFT–GGA results (circles and the dotted curve in Fig. 3), however, are somewhat surprising. The GGA gives positive δ with a minimum around 10 cm³/mol and δ increases quickly with decreasing V below this point. It can be estimated that SE works above 16 cm³/mol and DFT–GGA works below 8 cm³/mol. Apparently, neither method is adequate in the intermediate region between 8 and 16 cm³/mol. One can only speculate that δ behaves more or less monotonously, crossing over from negative values of the order of $3 \cdot 10^{-4}$ at higher volumes to the positive values at lower volumes, as shown schematically by the dashed line in Fig. 3.

The results for Kr and Xe are shown in Figs. 4 and 5, respectively. The results are qualitatively very similar to the case of Ar. Note that our DFT calculations clearly indicate positive δ at high pressures for Xe, in good agreement with the experiment [4,8] and the previous calculations [8,10], and in contradiction to Ref. 11. At $V = 8$ cm³/mol ($P \approx 300$ GPa), δ for Xe has a sharp maximum. It could be related to electronic topological transitions, but the detailed analysis of the electronic structure of the metallic phases is beyond the scope of the present paper.
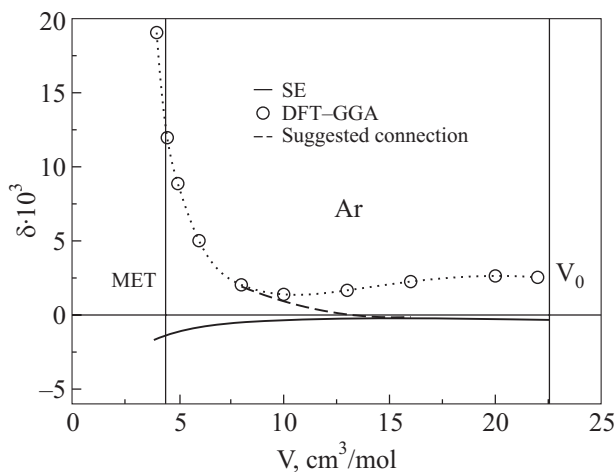

Fig. 4. The lattice distortion parameter δ for hcp krypton as a function of volume V from DFT–GGA and the SE potentials. The circles are calculated DFT–GGA points, while the smooth dotted curve is a cubic spline.
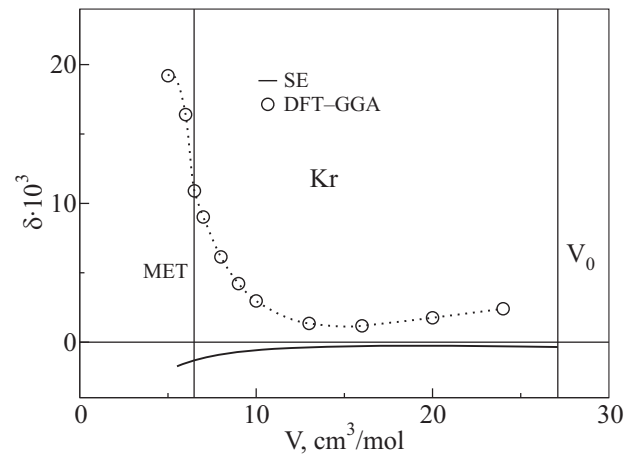
It is difficult to give a simple qualitative explanation to δ being negative for He under pressure, and positive for Ar, Kr, and Xe. Since helium has two $1s$ electrons, while Ar, Kr, and Xe have np^6 outermost shells, one can assume that this physical property is mainly determined by the quantum number l of the outermost electron shell (s or p) (the principal quantum number n seems irrelevant). It seems that the filled p shell favors positive δ under pressure, while the filled $1s$ shell of helium favors negative δ. Another possible explanation is that the heavier RGS's undergo metallization at much smaller pressures compared to helium. Note that the negative δ in helium rapidly decreases in absolute value in the metallic phase below 0.23 cm³/mol. So if we assume that the closeness to the metallization favours positive δ, it would explain the posi-

Fig. 3. The lattice distortion parameter δ for hcp argon as a function of volume V from DFT–GGA and the SE potentials. The circles are calculated DFT–GGA points, while the smooth dotted curve is a cubic spline.
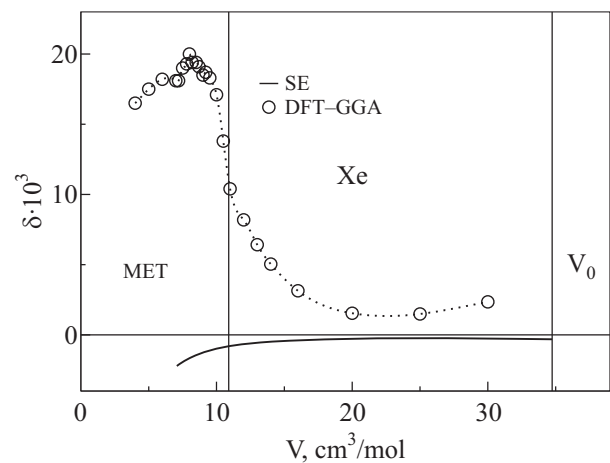

Fig. 5. The lattice distortion parameter δ for hcp xenon as a function of volume V from DFT–GGA and the SE potentials. The circles are calculated DFT–GGA points, while the smooth dotted curve is a cubic spline.

tive sign of δ in Ar, Kr, and Xe in the metallic phase and near the metallization, while in He the effect is too weak (with the metallization point at 0.228 cm^3/mol). In the language of *n*-body interactions, the pair forces are described well with the Aziz potential (with different parameters for different RGS's) and the 3-body potentials are likewise similar for He, Ar, Kr, and Xe. The triple forces always favour negative δ, while the pair forces give negative contribution to δ at larger volumes and positive at smaller volumes [6]. The total effect of pair and triple forces is always negative. Apparently, the distinction between He and the heavier RGS's manifests itself in 4-body and higher *n*-body terms, which are missing in our semi-empirical calculations; while GGA automatically includes all *n*-body terms.

4. Conclusion

We have calculated the lattice distortion parameter $\delta \equiv c/a - \sqrt{8/3}$ for the hcp rare gas solids He, Ar, Kr, and Xe. At low pressures (covered by the semi-empirical pair and 3-body potentials), δ is negative for all systems. At higher pressures (covered by DFT–GGA), δ becomes positive for Ar, Kr, and Xe, while it stays negative for helium.

1. P. Loubeyre, R. LeToullec, J.P. Pinceaux, H.K. Mao, J. Hu, and R.J. Hemley, *Phys. Rev. Lett*. **71**, 2272 (1993).

2. D. Errandonea, S. Boehler, R. Japel, M. Mezouar, and L.R. Benedetti, *Phys. Rev.* **B73**, 092106 (2006).

3. D. Errandonea, B. Schwager, R. Boehler, and M. Ross, *Phys. Rev.* **B65**, 214110 (2002).

4. A.P. Jephcoat, H.K. Mao, L.W. Finger, D.E. Cox, R.J. Hemley, and C.S. Zha, *Phys. Rev. Lett*. **59**, 2670 (1987).

5. A. Dewaele, F. Datchi, P. Loubeyre, and M. Mezouar, *Phys. Rev.* **B77**, 094106 (2008).

6. Yu.A. Freiman, S.M. Tretyak, A. Grechnev, A.F. Goncharov, J.S. Tse, D. Errandonea, H.K. Mao, and R.J. Hemley, *Phys. Rev.* **B80**, 094112 (2009).

7. J.V. Kranendonk, *Solid Hydrogen: Theory of the Properties of Solid H$_2$, HD, and* D$_2$, Plenum Press, New York (1983).

8. W.A. Caldwell, J.H. Nguyen, B.G. Pfrommer, F. Mauri, S.G. Louie, and R. Jeanloz, *Science* **277**, 930 (1997).

9. P. Schwerdtfeger, N. Gaston, R.P. Krawczyk, R. Tonner, and G.E. Moyano, *Phys. Rev.* **B73**, 064112 (2006).

10. Y. Yao and J.S. Tse, *Phys. Rev.* **B75**, 134104 (2007).

11. R.E. Cohen, L. Stixrude, and E. Wasserman, *Phys. Rev.* **B56**, 8575 (1997).

12. P. Loubeyre, *Phys. Rev. Lett*. **58**, 1857 (1987).

13. P. Loubeyre, *Phys. Rev.* **B37**, 5432 (1988).

14. Yu.A. Freiman and S.M. Tretyak, *Fiz. Nizk. Temp.* **33**, 719 (2007) [*Low Temp. Phys*. **33**, 545 (2007)].

15. P. Hohenberg and W. Kohn, *Phys. Rev.* **136**, B864 (1964).

16. W. Kohn and L. Sham, *Phys. Rev.* **140**, A1133 (1965).

17. J.K. Dewhurst, R. Ahuja, S. Li, and B. Johansson, *Phys. Rev. Lett*. **88**, 075504 (2002).

18. A. Tkachenko and O.A. von Lilienfeld, *Phys. Rev.* **B78**, 045116 (2008).

19. R.A. Aziz, V.P.S. Nain, J.S. Carley, W.L. Taylor, and G.T. McConville, *J. Chem. Phys.* **70**, 4330 (1979).

20. J.M. Wills, O. Eriksson, M. Alouani, and D.L. Price, in: *Electronic Structure and Physical Properties of Solids: The Uses of the LMTO Method*, Springer (2000).

21. The RSPT code homepage, *http://www.rspt.net*.

22. J.P. Perdew, K. Burke, and M. Ernzerhof, *Phys. Rev. Lett*. **77**, 3865 (1996).

23. C.A. Swenson, in: *Rare Gas Solids*, M.L. Klein and J.A. Venables (eds.), Academic Press, London (1976).

24. S.A. Khairallah and B. Militzer, *Phys. Rev. Lett*. **101**, 106407 (2008).

25. C. Kittel, *Introduction to Solid State Physics*, John Wiley & Sons (1996).